Common variants contribute to intrinsic functional architecture of human brain

Running title: GWAS of intrinsic brain function

Bingxin Zhao[1,14], Tengfei Li[2,3,14], Stephen M. Smith[4], Di Xiong[1], Xifeng Wang[1], Yue Yang[1], Tianyou Luo[1], Ziliang Zhu[1], Yue Shan[1], Mads E. Hauberg[5,6,8,9], Jaroslav Bendl[5-7], John F. Fullard[5-7], Panagiotis Roussos[5-7,10], Weili Lin[2,3], Yun Li[1,11,12], Jason L. Stein[11,13], and Hongtu Zhu[1,3]*

[1]Department of Biostatistics, University of North Carolina at Chapel Hill, Chapel Hill, NC, USA

[2]Department of Radiology, University of North Carolina at Chapel Hill, Chapel Hill, NC, USA

[3]Biomedical Research Imaging Center, School of Medicine, University of North Carolina at Chapel Hill, Chapel Hill, NC, USA

[4]Wellcome Centre for Integrative Neuroimaging, FMRIB, Nuffield Department of Clinical Neurosciences, University of Oxford, Oxford, UK

[5]Department of Psychiatry, Icahn School of Medicine at Mount Sinai, New York, NY, USA

[6]Friedman Brain Institute, Icahn School of Medicine at Mount Sinai, New York, NY, USA

[7]Department of Genetics and Genomic Science and Institute for Multiscale Biology, Icahn School of Medicine at Mount Sinai, New York, NY, USA

[8]iPSYCH, The Lundbeck Foundation Initiative for Integrative Psychiatric Research, Denmark

[9]Centre for Integrative Sequencing (iSEQ), Aarhus University, Aarhus, Denmark

[10]Mental Illness Research, Education, and Clinical Center (VISN 2 South), James J. Peters VA Medical Center, Bronx, NY, USA

[11]Department of Genetics, University of North Carolina at Chapel Hill, Chapel Hill, NC, USA

[12]Department of Computer Science, University of North Carolina at Chapel Hill, Chapel Hill, NC, USA

[13]UNC Neuroscience Center, University of North Carolina at Chapel Hill, Chapel Hill, NC, USA

[14]These authors contributed equally to this work.

Corresponding author:

Hongtu Zhu

3105C McGavran-Greenberg Hall, 135 Dauer Drive, Chapel Hill, NC 27599.

E-mail address: htzhu@email.unc.edu Phone: (919) 966-7250

Abstract

Human brain has a complex functional architecture and remains active during resting conditions. Resting-state functional magnetic resonance imaging (rsfMRI) measures brain activity at rest, which is closely linked with cognition and clinical outcomes. The role of genetics in human brain function is largely unknown. Here we utilized rsfMRI of 44,190 multi-ethnic individuals (37,339 in the UK Biobank) to discover the common genetic variants influencing intrinsic brain activity. We identified and validated hundreds of novel genetic loci associated with intrinsic functional signatures ($P < 2.8 \times 10^{-11}$), especially for interactions of the central executive, default mode, and salience networks involved in the triple network model of psychopathology. A number of intrinsic brain activity associated loci had been implicated with brain disorders (e.g., Alzheimer's disease, Parkinson's disease, schizophrenia) and cognition, such as 17q21.31, 19q13.32, and 2p16.1. Genetic correlation analysis suggested the shared genetic influences among intrinsic brain function, brain structure, and brain structural connectivity. We also detected significant genetic correlations with 26 other complex traits, such as education, cognitive performance, ADHD, major depressive disorder, schizophrenia, sleep, and neuroticism. Heritability of intrinsic brain activity was enriched in brain tissues. The reported risk genes of Alzheimer's disease typically had stronger associations with intrinsic brain activity than brain structure, and the associated genes of intrinsic brain activity were enriched in multiple biological pathways related to nervous system and neuropathology ($P < 1.8 \times 10^{-9}$).

Keywords: Amplitude; Functional Connectivity; Intrinsic brain activity; GWAS; Resting-state fMRI; Triple network model; UK Biobank.

Human brain is a complex system exhibiting a wide variety of neural activity and connectivity patterns across brain regions[1,2]. Functional organization and communication of brain networks are fundamental to bodily behavior and cognitive architectures[3-6]. Human brain remains active at rest, resulting in an intrinsic functional architecture. Utilizing changes in blood oxygen level-dependent (BOLD) signal[2,7], resting-state functional magnetic resonance imaging[8] (rsfMRI) can capture spontaneous intrinsic brain activity, or neuronal activity not attributable to a given task or stimulus[9]. Specifically, the spontaneous neuronal activity within each functional region can be quantified by the amplitude of low frequency fluctuations (ALFF) in BOLD time series[2,10,11]. Moreover, a functional connectivity matrix quantifying pairwise inter-regional correlations in spontaneous neuronal variability measures the magnitude of temporal synchrony between each pair of brain regions[2,12].

Several techniques have been developed to characterize functional brain regions and their interactions, such as seed-based analysis with prior knowledges[2,13], data-driven independent component analysis[14,15] (ICA), and graph methods[16]. The intrinsic brain activity patterns revealed in rsfMRI illuminate functional architecture of human brain[9]. For example, rsfMRI yields many insights into the resting-state networks (RSNs) of a healthy brain, such as default mode, central executive (i.e., frontoparietal), attention, limbic, salience, somatomotor, and visual networks[17-19]. These RSNs are strongly linked functional sub-networks[18,20] that commonly emerge in rsfMRI studies, which are of great interest in studies of cognition[21]. In addition, rsfMRI and RSNs have a wide range of clinical applications to detect brain abnormality in neurological and psychiatric disorders[13], such as Alzheimer's disease[22], Parkinson's disease[23], and major depressive disorder (MDD)[24]. Among these RSNs, the central executive, default mode, and salience networks are three core neurocognitive networks that support efficient cognition[25-27]. Accumulating evidence suggests that the functional organization and dynamic interaction of these three networks underlie a wide range of mental disorders, resulting in the triple network model of psychopathology[26,28].

Twin and family studies have largely reported a low to moderate degree of genetic contributions for intrinsic brain activity[29-35]. For example, the family-based heritability

estimates of major RSNs ranged from 20% to 40% in the Human Connectome Project (HCP)[36]. In a previous study using about 8,000 UK Biobank (UKB) individuals[37], the SNP heritability[38] of amplitude and functional connectivity traits can be more than 30%. Although there were multiple candidate gene studies for intrinsic brain activity (such as for *APOE*[39] and *KIBRA*[40]), currently only one genome-wide association study (GWAS)[37] has been successfully performed on rsfMRI[29] ($n \approx 8000$). This is mainly due to the fact that most rsfMRI datasets do not have enough participants for GWAS discovery and the overall genetic effects on neuronal activity are weaker compared to those on brain structure[37,41-45]. In addition, imaging batch effects[46] (e.g., image processing procedures, software) may cause substantial extra variability in rsfMRI analyses[47], making GWAS meta-analysis and independent replication particularly challenging. Therefore, genetic variants influencing intrinsic brain activity remain largely undiscovered and their shared genetic influences with other complex traits and clinical outcomes are unknown.

To address these challenges, here we collected individual-level rsfMRI data from four independent studies: the UK Biobank[48], Adolescent Brain Cognitive Development (ABCD[49]), Philadelphia Neurodevelopmental Cohort (PNC[50]), and HCP[51]. We harmonized rsfMRI processing procedures by following the unified UKB brain imaging pipeline[10,52]. Functional brain regions and corresponding functional connectivity were characterized via spatial ICA[53,54] for 44,190 multi-ethnic individuals, including 37,339 from UK Biobank. As in previous studies[10,37,55], two parcellations with different dimensionalities[18,56] (25 and 100 regions, respectively) were separately applied in spatial ICA and we focused on the 76 (21 and 55, respectively) regions that had been confirmed to be non-artefactual[10]. Two group of neuroimaging phenotypes were then generated: the first group contains 76 (node) amplitude traits reflecting the regional spontaneous neuronal activity; and the second group includes 1,695 (i.e., $21 \times 20/2 + 55 \times 54/2$) (edge) functional connectivity traits that quantify the inter-regional co-activity, as well as 6 global functional connectivity measures summarizing all of the 1,695 pairwise functional connectivity traits[37]. These 1,777 traits were then used to explore the genetic architecture of intrinsic brain activity. To aid interpretation of GWAS results, the functional brain regions characterized in ICA were labelled by using the automated anatomical labeling atlas[57] and were mapped onto major RSNs defined in Yeo, et al. [19]

and Finn, et al. [17]. Our GWAS results can be easily explored and downloaded through the Brain Imaging Genetics Knowledge Portal (BIG-KP) https://bigkp.web.unc.edu/.

RESULTS

Genetics of the intrinsic brain functional architecture.

SNP heritability was estimated for the 1,777 intrinsic brain activity traits via GCTA[58]. The mean heritability (h^2) estimate was 27.2% (range = (10%, 36.5%), standard error = 6.0%) for the 76 amplitude traits, all of which remained significant after adjusting for multiple comparisons by using the Benjamini-Hochberg procedure to control false discovery rate (FDR) at 0.05 level (1,777 tests, **Fig. 1a**, **Supplementary Table 1**). Among the 1,701 functional connectivity traits, 1,230 had significant (again at 5% FDR) heritability with estimates varying from 3% to 61% (mean = 9.6%, standard error = 5.8%). Ten functional connectivity traits had heritability larger than 30%, including 6 pairwise functional connectivity traits and 4 global functional connectivity measures. These traits were most related to central executive, default mode, and salience networks in the triple network model of psychopathology[26], indicating that the level of genetic control might be higher in these core neurocognitive networks (**Fig. 1b, Supplementary Fig. 1**). The range of heritability estimates was consistent with previous results[37], suggesting that common genetic variants had a low to moderate degree of contributions to inter-individual variability of intrinsic brain activity. The overall genetic effects on both amplitude and functional connectivity were lower than those on brain structure. For example, the average heritability was reported to be 48.7% for diffusion tensor imaging (DTI) traits of brain structural connectivity in white matter tracts[59] and 40% for regional brain volumes measuring brain morphometry[43]. However, as shown below, intrinsic brain activity may have stronger genetic connections with some brain disorders than brain structure, such as the Alzheimer's disease.

Genome-wide association discovery was carried out for 1,777 intrinsic brain activity traits using UKB individuals of British ancestry (n = 34,691, Methods). The Manhattan and QQ plots can be found in the BIG-KP server. At the significance level 2.8×10^{-11} (i.e., $5 \times 10^{-8}/1{,}777$, adjusted for the 1,777 traits), we identified 328 independent significant variants (linkage disequilibrium [LD] $r^2 < 0.2$, Methods) involved in 987 variant-trait

associations for 197 traits (75 amplitude and 122 functional connectivity, **Supplementary Table 2**). The amplitude traits typically had multiple associated variants (**Supplementary Table 3**) and a number of variants were widely related to the amplitude in different brain regions, such as rs11187837 in the 10q23.33 genomic region, rs9899649 in 17p11.2, rs10781575 in 10q26.3, and rs429358 in 19q13.32. For functional connectivity, rs2279829 in 3q24, rs2863957 in 2q14.1, rs7650184 in 3p11.1, and rs34522 in 5q14.3 were associated with multiple functional connectivity traits. Pairwise functional connectivity traits that had multiple significant variants were again most related to central executive, default mode, and salience networks (**Fig. 2a**). Of the 14 associated variants that had been identified in the previous GWAS[37], 12 were in LD ($r^2 \geq 0.6$) with our significant variants, most of which were associated with amplitude traits. With a more strict LD threshold (LD $r^2 < 0.1$), FUMA[60] selected 227 lead variants out of the 328 significant variants, and then characterized 604 significant locus-trait associations (Methods, **Fig. 2b**, **Supplementary Tables 4-5**). In summary, our analyses identify many novel variants associated with intrinsic functional signatures and illustrate the global genetic influences on functional connectivity across the whole brain. The degree of genetic control is higher in central executive, default mode, and salience networks, whose cross-network interactions closely control multiple cognitive functions and affect major brain disorders[28].

Validation and the effect of ethnicity.

We aimed to validate our results in UKB British GWAS using other independent datasets. First, we repeated GWAS on UKB individuals of White but Non-British ancestry (UKBW, n = 1,970). We found that 97.3% significant associations ($P < 2.8 \times 10^{-11}$) in UKB British GWAS had the same effect signs in the UKBW GWAS, and 82.5% had smaller P-values after meta-analyzing the two GWAS. These results suggest similar effect sizes and directions of the top variants among the European subjects within the UKB study[61,62]. Next, we performed GWAS in three non-UKB European cohorts: ABCD European (ABCDE, n = 3,821), HCP (n = 495), and PNC (n = 510). We meta-analyzed UKBW with the three non-UKB GWAS and checked whether the locus-trait associations detected in UKB British GWAS can be validated in the meta-analyzed validation GWAS (n = 6,796). For the 604 significant associations, 115 (19%) passed the 8.2×10^{-5} (i.e., 0.05/604)

Bonferroni significance level in this validation GWAS, and 599 (99.2%) were significant at FDR 5% level (**Supplementary Table 6**). Moreover, we performed a third meta-analysis to combine all of the five European GWAS, after which 75.5% significant associations in UKB British GWAS had smaller *P*-values. Overall, our results suggest that the associated genetic loci discovered in UKB British GWAS have high generalizability in independent European rsfMRI studies, despite the fact that these studies may use different imaging protocols/MRI scanners and recruit participants from different age groups. The good homogeneity of GWAS results may partially benefit from the consistent rsfMRI processing procedures that we applied to these datasets.

We further examined replication using polygenic risk scores[63] (PRS) derived from UKB British GWAS (Methods). For the 197 traits that had significant variants, 168 had significant PRS in at least one of the four European validation GWAS datasets at FDR 5% level (197 × 4 tests, **Supplementary Table 7**), illustrating the significant out-of-sample prediction power of our discovery GWAS results. The largest incremental R-squared were observed on the 2nd, 3rd, 4th, and 6th global functional connectivity measures in UKBW and HCP datasets, which were larger than 5% (range = (5.1%, 5.7%), *P* range = (1.1×10^{-24}, 4×10^{-13})). To evaluate the influences of ethnicity, PRS was also constructed on four non-European validation datasets: the UKB Asian (UKBA, n = 446), UKB Black (UKBBL, n = 232), ABCD Hispanic (ABCDH, n = 768), and ABCD African American (ABCDA, n = 1,257). UKBA had the best validation performance among the four datasets, with 86 PRS being significant at FDR 5% level (197 × 4 tests, **Supplementary Table 7**). The number of significant PRS was reduced to 59, 39, and 31 in ABCDH, ABCDA, and UKBBL, respectively. In summary, these PRS results illustrate the overall consistency of genetic effects in European cohorts and also show the potential negative effects of ethnicity in cross-population applications, especially for Black/African-American cohorts. More efforts are required to identify further loci associated with functional brain in global diverse populations.

The shared genetic loci with brain-related complex traits and disorders.

To evaluate the shared genetic influences between intrinsic brain activity and other complex traits, we carried out association lookups for the 328 significant variants (and

their LD tags, i.e., variants with LD $r^2 \geq 0.6$) detected in UKB British GWAS (Methods). On the NHGRI-EBI GWAS catalog[64], our results tagged many variants reported for a wide range of complex traits in different trait domains, such as cognitive performance, neurological and psychiatric disorders, education, bone mineral density, sleep, smoking/drinking, brain structure, and anthropometric traits (**Supplementary Table 8**). Below we highlighted colocalizations in a few selected genomic regions.

The 17q21.31 region was associated with functional connectivity of temporal and frontal regions mostly involved in central executive, default mode, and salience networks (**Fig. 3a**). This genomic region has been reported by Parkinson's disease studies[65-69]. As a system-level progressive neurodegenerative disorder[70], Parkinson's disease not only led to motor abnormalities, but also had non-motor symptoms such as temporal perception abnormalities[71] and impaired connectivity among frontal regions[72]. Cognitive dysfunction and disrupted coupling between default mode and salience networks were commonly reported in Parkinson's disease[27]. In addition to Parkinson's disease, the 17q21.31 region was widely related to other complex traits, including neurological disorders (e.g., Alzheimer's disease[73], corticobasal degeneration[74], progressive supranuclear palsy[75]), psychiatric disorders (e.g., autism spectrum disorder[76], depressive symptoms[77]), educational attainment[78,79], psychological traits (e.g., neuroticism[77]), cognitive traits (cognitive ability[80]), sleep[81], heel bone mineral density[82], alcohol use disorder[83], subcortical brain volumes[44], and white matter microstructure[59].

Next, the 19q13.32 region had genetic effects on the amplitude of many functional brain regions that were most in default mode, central executive (i.e., frontoparietal), attention, and visual networks (**Fig. 3b**). It is well known that 19q13.32 is a risk locus of Alzheimer's disease, containing genes such as *APOE, APOC,* and *TOMM40*. In this region, we tagged variants associated with dementia and decline in mental ability, including Alzheimer's disease[84-88], frontotemporal dementia[89], cerebral amyloid angiopathy[90], cognitive decline[91-93], cognitive impairment test score[94], as well as many biomarkers of Alzheimer's disease, such as neurofibrillary tangles[90], neuritic plaque[90], cerebral amyloid deposition[95], cerebrospinal fluid protein levels[94], and cortical amyloid beta load[88]. Altered amplitude activity has been widely reported in patients of cognitive impairment

and Alzheimer's disease[96,97]. The brain degeneration related to Alzheimer's disease may begin in the frontoparietal regions[98] and was associated with dysfunction of multiple RSNs, especially the default mode network[22]. Our findings suggest the shared genetic influences between intrinsic neuronal activity and brain atrophy of Alzheimer's disease.

In addition, the 2p16.1 and 5q15 regions were mainly associated with interactions among central executive, default mode, and salience networks (**Fig. 3c**, **Fig. 3d**, and **Supplementary Fig. 2**). We observed colocalizations with psychiatric disorders (e.g., schizophrenia[99], MDD[100], depressive symptoms[101], autism spectrum disorder[102]), psychological traits (e.g., neuroticism[77], well-being spectrum[103]), sleep[104], cognitive traits (e.g., intelligence[105]), and hippocampus subfield volumes[106]. Dysregulated triple network interactions were frequently reported in patients of schizophrenia[107], depression[108], and autism spectrum disorder[109]. Similarly, the 2q24.2 and 10q26.13 regions had genetic effects on functional connectivity traits involved in central executive, default mode, salience, and attention networks (**Supplementary Figs. 3-4**). In these two regions, our identified variants tagged those that have been implicated with schizophrenia[110], educational attainment[78], cognitive traits (e.g., cognitive ability[80]), smoking/drinking (e.g., smoking status[79,111], alcohol consumption[111]), hippocampus subfield volumes[106], and heel bone mineral density[82]. We also observed colocalizations in many other genomic regions, such as in 2q14.1 region with sleep traits (e.g., sleep duration[81,112], insomnia[104]), in 3p11.1 with cognitive traits (e.g., cognitive ability[113], intelligence[114], math ability[78]), in 2p21 with heel bone mineral density[79,115], and in 6p25.3 with stroke[116,117]. In summary, instinct brain function has wide genetic links to a large number of brain-related complex traits and clinical outcomes, especially the neurological and psychiatric disorders and cognitive traits.

Genetic correlations with brain structure and cognition.

To explore whether genetically mediated brain structural changes were associated with brain function, we examined pairwise genetic correlations (gc) between 82 intrinsic brain activity traits (i.e., the 76 amplitude traits and the 6 global functional connectivity measures) and 315 traits of brain structure via LDSC[118] (Methods), including 100 regional brain volumes[43] and 215 DTI traits of brain structural connectivity in white

matter tracts[119]. There were 137 significant pairs between 44 intrinsic brain functional traits and 87 brain structural traits at FDR 5% level (82 × 315 tests, |gc| range = (0.18, 0.44), *P* range = (4.3×10^{-12}, 2.6×10^{-4}), **Supplementary Table 9**).

We found significant genetic correlations between global functional connectivity measures and regional volumes in cerebral cortex, including prefrontal (caudal middle frontal, pars orbitalis, pars triangularis) and precentral of frontal lobe; superolateral (inferior parietal, supramarginal) and postcentral of parietal lobe; superolateral (transverse temporal, middle temporal, superior temporal) of temporal lobe; and insula (|gc| range = (0.2, 0.42), $P < 1.4 \times 10^{-4}$**, Fig. 4a**). These global functional connectivity measures mainly represented the central executive, default mode, salience, and attention networks, suggesting the widely shared genetic influences between cerebral cortex volumes and cognation. Amplitude traits also had significant genetic correlations with brain volumes, most of which were negative. For example, 16 amplitude traits across multiple RSNs had significant genetic correlations with total brain volume (|gc| range = (0.2, 0.41), $P < 2 \times 10^{-4}$). It is well known that brain size/volume is phenotypically associated with intrinsic amplitude[120]. Moreover, the amplitude of putamen and caudate regions in subcortical-cerebellum network[17] was genetically correlated with ventricular volumes (|gc| range = (0.26, 0.36), $P < 5.9 \times 10^{-5}$). Ventricular volumes are known to be related to subcortical volumes[121,122]. For the amplitude of precuneus region in default mode and central executive networks, we observed significant genetic correlations with cuneus, lingual, and pericalcarine volumes in occipital lobe (|gc| range = (0.2, 0.37), $P < 1 \times 10^{-4}$). In addition, the amplitude of occipital regions (calcarine, lingual, and cuneus) in visual network had significant genetic correlations with pericalcarine volume (|gc| range = (0.3, 0.44), $P < 5.1 \times 10^{-5}$). Cerebral cortex is deeply involved in a wide variety of brain function[19,123]. Our results uncover the genetic links between intrinsic brain function and the associated structural substrates.

Significant genetic correlations were also observed between intrinsic brain activity and brain structural connectivity (**Fig. 4b**). We highlighted the amplitude of frontal regions (precentral, middle/inferior frontal) in central executive network, which had significant genetic correlations with global integrity of white matter and tract-specific integrity in

body of corpus callosum (BCC), cingulum cingulate gyrus (CGC), external capsule (EC), long anterior limb of internal capsule (ALIC), posterior limb of internal capsule (RLIC), and superior longitudinal fasciculus (SLF) tracts (|gc| range = (0.2, 0.29), $P < 2.5 \times 10^{-4}$). Another example is the amplitude of occipital and temporal regions (middle occipital, inferior/middle temporal) in visual and attention networks, which was genetically correlated with the structural connectivity in BCC, fornix (FX), superior corona radiata (SCR), posterior corona radiata (PCR), posterior limb of internal capsule (PLIC), RLIC, and SLF tracts (|gc| range = (0.22, 0.37), $P < 2.4 \times 10^{-4}$). In addition, global functional connectivity measures were genetically correlated with BCC, genu of corpus callosum (GCC), splenium of corpus callosum (SCC), EC, posterior thalamic radiation (PTR), SLF, uncinate fasciculus (UNC), corticospinal tract (CST), and sagittal stratum (SS) tracts (|gc| range = (0.18, 0.41), $P < 2.2 \times 10^{-4}$). Structural connectivity and functional connectivity have a complex but close relationship[20,124], and our analyses provide new insights into their genetic overlaps. To our knowledge, these results are the first to indicate that genetic changes in brain structure may also impact intrinsic brain function and result in brain functional differences.

Next, we examined the genetic correlations between 1,777 intrinsic brain activity traits and 30 other complex traits, mainly focusing on cognition and brain disorders (**Supplementary Table 10**). We found 176 significant pairs between 26 complex traits and 102 intrinsic brain activity traits at FDR 5% level (30 × 1,777 tests, P range = (8.6×10^{-12}, 2.3×10^{-3}), **Supplementary Table 11**). For amplitude traits, we detected significant genetic correlations with cognitive traits studied in previous GWAS, including cognitive performance, general cognitive function, intelligence, and numerical reasoning (|gc| range = (0.15, 0.21), $P < 1.8 \times 10^{-4}$, **Fig. 5**). We also observed significant genetic correlations with cross disorder (five major psychiatric disorders[125]) (|gc| range = (0.32, 0.33), $P < 9.7 \times 10^{-5}$) and sleep (|gc| range = (0.15, 0.18), $P < 1.6 \times 10^{-4}$). The association between intrinsic amplitude and cognition[21], sleep[126], and brain disorders[127] had been previously reported. Furthermore, many significant genetic correlations were uncovered between intrinsic functional connectivity and brain-related traits, such as education, cognitive traits, cross disorder, attention-deficit/hyperactivity disorder (ADHD), schizophrenia, MDD, neuroticism, sleep, risk tolerance, and subjective well-being. For

example, ADHD was genetically correlated with functional connectivity in attention, somatomotor, and subcortical-cerebellum networks (|gc| = 0.31, $P = 1.2 \times 10^{-4}$), and MDD had significant genetic correlations with default mode, central executive, and salience networks (|gc| range = (0.26, 0.27), $P < 1.2 \times 10^{-4}$) (**Supplementary Fig. 5**). In addition, many functional connectivity traits across major RSNs had genetic correlations with education (|gc| range = (0.14, 0.35), $P < 1.8 \times 10^{-4}$), cognitive performance (|gc| range = (0.15, 0.35), $P < 1.3 \times 10^{-4}$), cross disorder (|gc| range = (0.26, 0.37), $P < 8.7 \times 10^{-5}$), and schizophrenia (|gc| range = (0.18, 0.3), $P < 1.2 \times 10^{-4}$), matching previously reported phenotypical associations[55,107,109] (**Supplementary Figs. 6-8**). We also found broad genetic correlations with manual occupation[128] (|gc| range = (0.15, 0.24), $P < 1.5 \times 10^{-4}$), BMI[129] (|gc| range = (0.2, 0.37), $P < 1.5 \times 10^{-4}$), and behavioral factors (drinking[130] and smoking[131]), all of which had been linked to brain functional differences.

Gene-level association analysis and biological annotations.

Gene-level association was tested via MAGMA[132] (Methods), which detected 970 significant gene-trait associations ($P < 1.5 \times 10^{-9}$, adjusted for 1,777 phenotypes) for 123 genes (**Supplementary Fig. 9, Supplementary Table 12**). In addition, we applied FUMA[60] to map significant variants ($P < 2.8 \times 10^{-11}$) to genes via physical position, expression quantitative trait loci (eQTL) association, and 3D chromatin (Hi-C) interaction, which yielded 273 more associated genes that were not discovered in MAGMA (352 in total, **Supplementary Table 13**). For the 396 genes associated with intrinsic brain activity in either MAGMA or FUMA, 89 had been linked to white matter microstructure[119], 52 were reported to be associated with regional brain volumes[43], and 43 were related to both of them (**Supplementary Table 14**). These triple overlapped genes were also widely associated with other complex traits, such as Parkinson's disease, neuroticism, alopecia, handedness, reaction time, and intelligence (**Supplementary Table 15**), providing more insights into the genetic overlaps among brain structure, brain function, and other brain-related traits. For example, *MAPT, NSF, WNT3, CRHR1, PLEKHM1, STH, LRRC37A3, ARHGAP27, KANSL1*, and *SPPL2C* were risk genes of Parkinson's disease, which were also associated with pallidum grey matter volume[43], fractional anisotropy and mean diffusivity of white matter microstructure[119], and intrinsic functional connectivity in central executive, default mode, and salience networks. These complementary

neuroimaging traits had all been used to study the pathophysiology of Parkinson's disease[133-135]. In addition, 5 of our intrinsic brain activity associated genes (*CALR, CALY, SLC47A1, CYP2C8, CYP2C9*) were targets for 12 nervous system drugs[136], such as 5 psycholeptics (ATC code: N05) to produce calming effects, 2 anti-depressants (N06A) to treat MDD and related conditions, 2 anti-migraine (N02C), and one anti-dementia (N06D) (**Supplementary Table 16**).

It is of particular interest to study the functional connectivity dysfunction in Alzheimer's disease and identify the overlapped genes[22,137]. Our gene-level analysis replicated *APOE* and *SORL1*, which were frequently targeted in Alzheimer's disease-candidate gene studies of functional connectivity[29,138]. More importantly, we uncovered more overlapped genes between intrinsic brain activity and Alzheimer's disease, such as *PVRL2, TOMM40, APOC1, MAPK7, CLPTM1, HESX1, BCAR3, ANO3*, and *YAP1* (**Supplementary Table 17**). These genes had much stronger associations with intrinsic brain activity than brain structure. We also found many pleiotropic genes associated with serum metabolite, low density lipoprotein cholesterol, high density lipoprotein cholesterol, triglyceride, type II diabetes mellitus, and blood protein measurements, all of which might be related to the Alzheimer's disease[139,140]. These results largely expand the overview of the shared genetic components among metabolic dysfunction, blood biomarkers, brain function, and Alzheimer's disease, suggesting the potential value of integrating these traits in future Alzheimer's disease research.

To identify the tissues and cell types in which genetic variation yields differences in functional connectivity, we performed partitioned heritability analyses[141] for tissue type and cell type specific regulatory elements[142] (Methods). We focused on the 10 functional connectivity traits that had heritability larger than 30%. At FDR 5% level, the most significant enrichments of heritability were observed in active gene regulation regions of fetal brain tissues, neurospheres, and neuron/neuronal progenitor cultured cells (**Supplementary Fig. 10, Supplementary Table 18**). We also tried to further identify brain cell type specific enrichments using chromatin accessibility data of two main gross brain cell types[143] (i.e., neurons (NeuN+) and glia (NeuN-)) and multiple neuronal and glial cell subtypes, including oligodendrocyte (NeuN-/Sox10+), microglia, and astrocyte

(NeuN-/Sox10-), as well as GABAergic (NeuN+/Sox6+) and glutamatergic neurons (NeuN+/Sox6-). No significant enrichment was detected for these brain cell types after adjusting for multiple testing. Next, we performed MAGMA tissue-specific gene property[132] analysis for 13 GTEx[144] (v8) brain tissues (Methods). We found that genes with higher expression levels in human brain tissues generally had stronger associations with intrinsic brain activity, particularly for tissues sampled from cerebellar hemisphere and cerebellum regions ($P < 1.9 \times 10^{-5}$, **Supplementary Fig. 11**, **Supplementary Table 19**).

MAGMA[132] gene-set analysis was performed to prioritize the enriched biological pathways (Methods). We found 59 significantly enriched gene sets after Bonferroni adjustment ($P < 1.8 \times 10^{-9}$, **Supplementary Table 20**). Multiple pathways related to nervous system were detected, such as “go neurogenesis” (GO: 0022008), “go neuron differentiation” (GO: 0030182), “go regulation of nervous system development” (GO: 0051960), “go regulation of neuron differentiation” (GO: 0045664), “go cell morphogenesis involved in neuron differentiation” (GO: 0048667), and “go neuron development” (GO: 0048666). Other frequently prioritized gene sets included “dacosta uv response via ercc3 dn” (M4500), “go dna binding transcription factor activity” (GO:0003700), “go sequence specific dna binding” (GO:0043565), “dacosta uv response via ercc3 common dn” (M13522), “go negative regulation of rna biosynthetic process” (GO:1902679), “go negative regulation of biosynthetic process” (GO:0009890), and “go regulatory region nucleic acid binding” (GO: 0001067). M4500 and M13522 are *ERCC3*-associated gene sets related to xeroderma pigmentosum (XP) and trichothiodystrophy (TTD) syndromes[145,146]. The *ERCC3* gene was highly relevant to the progression of Alzheimer's disease[147]. Patients affected with XP or TTD may have primary neuronal degeneration and reduced myelination[146], which were closely related to abnormal functional connectivity[148] and intellectual impairment[149].

DISCUSSION

In the present study, we evaluated the influences of common variants on intrinsic brain functional architecture using uniformly processed rsfMRI data of 44,190 subjects from four independent studies. Genome-wide association analysis found hundreds of novel

loci related to intrinsic brain activity in the UKB British cohort, which were successfully replicated in independent datasets. The interactions across core neurocognitive networks (central executive, default mode, and salience) in the triple network model had genetic links with cognation and multiple brain disorders. The shared genetic factors among functional, structural, and diffusion neuroimaging traits were also uncovered. Gene-level analysis detected many overlapped genes between intrinsic brain activity and Alzheimer's disease. The enriched tissues and biological pathways were also prioritized in bioinformatic analyses. Compared to the previous study[37] with about 8,000 subjects, this large-scale GWAS much improved our understanding of the genetic architecture of functional human brain.

Our study faces a few limitations. First, the samples in our discovery GWAS were mainly from European ancestry. In our PRS analysis, we illustrated the negative effects of ethnicity when applying the European GWAS results on validation cohorts with non-European ancestry. The multi-ethnic genetic architecture of intrinsic brain activity needs to be further investigated when more rsfMRI data from global populations become available. Second, our study focused on the brain functional activity at rest. Recent study[34] had found that combining rsfMRI and task functional magnetic resonance imaging (tfMRI) may result in higher heritability estimates and potentially boost the GWAS power. Thus, future studies could model rsfMRI and tfMRI together to uncover more insights into the genetic influences on brain function. In addition, we applied ICA in this study, which was a popular data-driven approach to characterize the functionally connected brain[2]. It is also of great interest to evaluate the performance of other popular rsfMRI approaches (such as seed-based analysis and graph theory) in these large-scale datasets. Finally, although we found the genetic links between brain function and other complex traits, the shared biological mechanisms and causal genetic relationships among these traits remain largely unclear. More efforts are required to enhance our knowledge of human brain using the accumulating publicly available imaging genetics data resources.

URLs.

Brain Imaging GWAS Summary Statistics, https://github.com/BIG-S2/GWAS;

Brain Imaging Genetics Knowledge Portal, https://bigkp.web.unc.edu/;

UKB Imaging Pipeline, https://git.fmrib.ox.ac.uk/falmagro/UK_biobank_pipeline_v_1;

PLINK, https://www.cog-genomics.org/plink2/;

GCTA & fastGWA, http://cnsgenomics.com/software/gcta/;

METAL, https://genome.sph.umich.edu/wiki/METAL;

FUMA, http://fuma.ctglab.nl/;

MGAMA, https://ctg.cncr.nl/software/magma;

LDSC, https://github.com/bulik/ldsc/;

FINDOR, https://github.com/gkichaev/FINDOR;

NHGRI-EBI GWAS Catalog, https://www.ebi.ac.uk/gwas/home;

The atlas of GWAS Summary Statistics, http://atlas.ctglab.nl/.

METHODS

Methods are available in the ***Methods*** section.

Note: One supplementary information pdf file and one supplementary table zip file are available.

ACKNOWLEDGEMENTS

This research was partially supported by U.S. NIH grants MH086633 (H.Z.) and MH116527 (TF.L.). We thank the individuals represented in the UK Biobank, ABCD, HCP, and PNC studies for their participation and the research teams for their work in collecting, processing and disseminating these datasets for analysis. We gratefully acknowledge all the studies and databases that made GWAS summary data available. This research has been conducted using the UK Biobank resource (application number 22783), subject to a data transfer agreement. Part of the data used in the preparation of this article were obtained from the Adolescent Brain Cognitive Development (ABCD) Study (https://abcdstudy.org), held in the NIMH Data Archive (NDA). This is a multisite, longitudinal study designed to recruit more than 10,000 children age 9-10 and follow them over 10 years into early adulthood. The ABCD Study is supported by the National Institutes of Health and additional federal partners under award numbers U01DA041022, U01DA041028, U01DA041048, U01DA041089, U01DA041106, U01DA041117, U01DA041120, U01DA041134, U01DA041148, U01DA041156,

U01DA041174, U24DA041123, U24DA041147, U01DA041093, and U01DA041025. A full list of supporters is available at https://abcdstudy.org/federal-partners.html. A listing of participating sites and a complete listing of the study investigators can be found at https://abcdstudy.org/scientists/workgroups/. ABCD consortium investigators designed and implemented the study and/or provided data but did not necessarily participate in analysis or writing of this report. This manuscript reflects the views of the authors and may not reflect the opinions or views of the NIH or ABCD consortium investigators. Support for the collection of the PNC datasets was provided by grant RC2MH089983 awarded to Raquel Gur and RC2MH089924 awarded to Hakon Hakonarson. All PNC subjects were recruited through the Center for Applied Genomics at The Children's Hospital in Philadelphia. HCP data were provided by the Human Connectome Project, WU-Minn Consortium (Principal Investigators: David Van Essen and Kamil Ugurbil; 1U54MH091657) funded by the 16 NIH Institutes and Centers that support the NIH Blueprint for Neuroscience Research; and by the McDonnell Center for Systems Neuroscience at Washington University.

AUTHOR CONTRIBUTIONS

B.Z., H.Z., J.L.S., W.L., and Y.L. designed the study. B.Z., TF.L., D.X., X.W., Y.Y., and TY.L. analyzed the data. TF. L., Z.Z., and Y.S. downloaded the datasets, processed rsfMRI data, and undertook quantity controls. P.R., M.E.H., J.B., and J.F.F. analyzed brain cell chromatin accessibility data. B.Z. and H.Z. wrote the manuscript with feedback from all authors.

CORRESPINDENCE AND REQUESTS FOR MATERIALS should be addressed to H.Z.

COMPETETING FINANCIAL INTERESTS

The authors declare no competing financial interests.

REFERENCES

1. Avena-Koenigsberger, A., Misic, B. & Sporns, O. Communication dynamics in complex brain networks. *Nature Reviews Neuroscience* **19**, 17 (2018).

2. Lv, H. *et al.* Resting-state functional MRI: everything that nonexperts have always wanted to know. *American Journal of Neuroradiology* **39**, 1390-1399 (2018).
3. Petersen, S.E. & Sporns, O. Brain networks and cognitive architectures. *Neuron* **88**, 207-219 (2015).
4. Park, H.-J. & Friston, K. Structural and functional brain networks: from connections to cognition. *Science* **342**(2013).
5. Medaglia, J.D., Lynall, M.-E. & Bassett, D.S. Cognitive network neuroscience. *Journal of cognitive neuroscience* **27**, 1471-1491 (2015).
6. van den Heuvel, M.P. & Sporns, O. Network hubs in the human brain. *Trends in cognitive sciences* **17**, 683-696 (2013).
7. Fox, M.D. & Greicius, M. Clinical applications of resting state functional connectivity. *Frontiers in systems neuroscience* **4**, 19 (2010).
8. Biswal, B., Zerrin Yetkin, F., Haughton, V.M. & Hyde, J.S. Functional connectivity in the motor cortex of resting human brain using echo-planar MRI. *Magnetic resonance in medicine* **34**, 537-541 (1995).
9. Fox, M.D. & Raichle, M.E. Spontaneous fluctuations in brain activity observed with functional magnetic resonance imaging. *Nature reviews neuroscience* **8**, 700-711 (2007).
10. Alfaro-Almagro, F. *et al.* Image processing and Quality Control for the first 10,000 brain imaging datasets from UK Biobank. *NeuroImage* **166**, 400-424 (2018).
11. Jia, X.-Z. *et al.* Percent amplitude of fluctuation: a simple measure for resting-state fMRI signal at single voxel level. *Plos one* **15**, e0227021 (2020).
12. Hutchison, R.M. *et al.* Dynamic functional connectivity: promise, issues, and interpretations. *Neuroimage* **80**, 360-378 (2013).
13. Lee, M.H., Smyser, C.D. & Shimony, J.S. Resting-state fMRI: a review of methods and clinical applications. *American Journal of neuroradiology* **34**, 1866-1872 (2013).
14. Beckmann, C.F., DeLuca, M., Devlin, J.T. & Smith, S.M. Investigations into resting-state connectivity using independent component analysis. *Philosophical Transactions of the Royal Society B: Biological Sciences* **360**, 1001-1013 (2005).
15. Damoiseaux, J.S. *et al.* Consistent resting-state networks across healthy subjects. *Proceedings of the national academy of sciences* **103**, 13848-13853 (2006).

16. Grayson, D.S. & Fair, D.A. Development of large-scale functional networks from birth to adulthood: A guide to the neuroimaging literature. *Neuroimage* **160**, 15-31 (2017).
17. Finn, E.S. *et al.* Functional connectome fingerprinting: identifying individuals using patterns of brain connectivity. *Nature neuroscience* **18**, 1664-1671 (2015).
18. Smith, S.M. *et al.* Correspondence of the brain's functional architecture during activation and rest. *Proceedings of the national academy of sciences* **106**, 13040-13045 (2009).
19. Yeo, B.T. *et al.* The organization of the human cerebral cortex estimated by intrinsic functional connectivity. *Journal of neurophysiology* (2011).
20. Van Den Heuvel, M.P. & Pol, H.E.H. Exploring the brain network: a review on resting-state fMRI functional connectivity. *European neuropsychopharmacology* **20**, 519-534 (2010).
21. Fryer, S.L. *et al.* Relating intrinsic low-frequency BOLD cortical oscillations to cognition in schizophrenia. *Neuropsychopharmacology* **40**, 2705-2714 (2015).
22. Badhwar, A. *et al.* Resting-state network dysfunction in Alzheimer's disease: a systematic review and meta-analysis. *Alzheimer's & Dementia: Diagnosis, Assessment & Disease Monitoring* **8**, 73-85 (2017).
23. Wolters, A.F. *et al.* Resting-state fMRI in Parkinson's disease patients with cognitive impairment: A meta-analysis. *Parkinsonism & Related Disorders* **62**, 16-27 (2019).
24. Mulders, P.C., van Eijndhoven, P.F., Schene, A.H., Beckmann, C.F. & Tendolkar, I. Resting-state functional connectivity in major depressive disorder: a review. *Neuroscience & Biobehavioral Reviews* **56**, 330-344 (2015).
25. Menon, V. & Uddin, L.Q. Saliency, switching, attention and control: a network model of insula function. *Brain Structure and Function* **214**, 655-667 (2010).
26. Menon, V. Large-scale brain networks and psychopathology: a unifying triple network model. *Trends in cognitive sciences* **15**, 483-506 (2011).
27. Putcha, D., Ross, R.S., Cronin-Golomb, A., Janes, A.C. & Stern, C.E. Salience and default mode network coupling predicts cognition in aging and Parkinson's disease. *Journal of the International Neuropsychological Society: JINS* **22**, 205 (2016).

28. Menon, V. The triple network model, insight, and large-scale brain organization in autism. *Biological psychiatry* **84**, 236 (2018).
29. Foo, H. *et al.* Genetic influence on ageing-related changes in resting-state brain functional networks in healthy adults: a systematic review. *Neuroscience & Biobehavioral Reviews* (2020).
30. Teeuw, J. *et al.* Genetic and environmental influences on functional connectivity within and between canonical cortical resting-state networks throughout adolescent development in boys and girls. *NeuroImage* **202**, 116073 (2019).
31. Meda, S.A. *et al.* Multivariate analysis reveals genetic associations of the resting default mode network in psychotic bipolar disorder and schizophrenia. *Proceedings of the National Academy of Sciences* **111**, E2066-E2075 (2014).
32. Duncan, L. *et al.* Analysis of polygenic risk score usage and performance in diverse human populations. *Nature communications* **10**, 1-9 (2019).
33. Glahn, D. *et al.* Genetic control over the resting brain. *Proceedings of the National Academy of Sciences* **107**, 1223-1228 (2010).
34. Elliott, M.L. *et al.* General functional connectivity: Shared features of resting-state and task fMRI drive reliable and heritable individual differences in functional brain networks. *NeuroImage* **189**, 516-532 (2019).
35. Ge, T., Holmes, A.J., Buckner, R.L., Smoller, J.W. & Sabuncu, M.R. Heritability analysis with repeat measurements and its application to resting-state functional connectivity. *Proceedings of the National Academy of Sciences* **114**, 5521-5526 (2017).
36. Adhikari, B.M. *et al.* Heritability estimates on resting state fMRI data using ENIGMA analysis pipeline. (2018).
37. Elliott, L.T. *et al.* Genome-wide association studies of brain imaging phenotypes in UK Biobank. *Nature* **562**, 210-216 (2018).
38. Yang, J., Zeng, J., Goddard, M.E., Wray, N.R. & Visscher, P.M. Concepts, estimation and interpretation of SNP-based heritability. *Nature Genetics* **49**, 1304-1310 (2017).
39. Chiesa, P.A. *et al.* Revolution of resting-state functional neuroimaging genetics in Alzheimer's disease. *Trends in neurosciences* **40**, 469-480 (2017).

40. Zhang, N. *et al.* APOE and KIBRA interactions on brain functional connectivity in healthy young adults. *Cerebral Cortex* **27**, 4797-4805 (2017).
41. Satizabal, C.L. *et al.* Genetic architecture of subcortical brain structures in 38,851 individuals. *Nature genetics* **51**, 1624-1636 (2019).
42. Grasby, K.L. *et al.* The genetic architecture of the human cerebral cortex. *Science* **367**(2020).
43. Zhao, B. *et al.* Genome-wide association analysis of 19,629 individuals identifies variants influencing regional brain volumes and refines their genetic co-architecture with cognitive and mental health traits. *Nature Genetics* **51**, 1637-1644 (2019).
44. Hibar, D.P. *et al.* Common genetic variants influence human subcortical brain structures. *Nature* **520**, 224-229 (2015).
45. Stein, J.L. *et al.* Identification of common variants associated with human hippocampal and intracranial volumes. *Nature Genetics* **44**, 552-561 (2012).
46. Smith, S.M. & Nichols, T.E. Statistical challenges in "big data" human neuroimaging. *Neuron* **97**, 263-268 (2018).
47. Botvinik-Nezer, R. *et al.* Variability in the analysis of a single neuroimaging dataset by many teams. *Nature*, 1-7 (2020).
48. Sudlow, C. *et al.* UK biobank: an open access resource for identifying the causes of a wide range of complex diseases of middle and old age. *PLoS Medicine* **12**, e1001779 (2015).
49. Casey, B. *et al.* The adolescent brain cognitive development (ABCD) study: imaging acquisition across 21 sites. *Developmental cognitive neuroscience* **32**, 43-54 (2018).
50. Satterthwaite, T.D. *et al.* Neuroimaging of the Philadelphia neurodevelopmental cohort. *Neuroimage* **86**, 544-553 (2014).
51. Somerville, L.H. *et al.* The Lifespan Human Connectome Project in Development: A large-scale study of brain connectivity development in 5–21 year olds. *NeuroImage* **183**, 456-468 (2018).
52. Miller, K.L. *et al.* Multimodal population brain imaging in the UK Biobank prospective epidemiological study. *Nature Neuroscience* **19**, 1523-1536 (2016).

53. Beckmann, C.F. & Smith, S.M. Probabilistic independent component analysis for functional magnetic resonance imaging. *IEEE transactions on medical imaging* **23**, 137-152 (2004).
54. Hyvarinen, A. Fast and robust fixed-point algorithms for independent component analysis. *IEEE transactions on Neural Networks* **10**, 626-634 (1999).
55. Shen, X. *et al.* Resting-state connectivity and its association with cognitive performance, educational attainment, and household income in the UK Biobank. *Biological Psychiatry: Cognitive Neuroscience and Neuroimaging* **3**, 878-886 (2018).
56. Smith, S.M. *et al.* Resting-state fMRI in the human connectome project. *Neuroimage* **80**, 144-168 (2013).
57. Rolls, E.T., Huang, C.-C., Lin, C.-P., Feng, J. & Joliot, M. Automated anatomical labelling atlas 3. *NeuroImage* **206**, 116189 (2020).
58. Yang, J., Lee, S.H., Goddard, M.E. & Visscher, P.M. GCTA: a tool for genome-wide complex trait analysis. *The American Journal of Human Genetics* **88**, 76-82 (2011).
59. Zhao, B. *et al.* Large-scale GWAS reveals genetic architecture of brain white matter microstructure and genetic overlap with cognitive and mental health traits (n = 17,706). *Molecular Psychiatry* (2019).
60. Watanabe, K., Taskesen, E., Bochoven, A. & Posthuma, D. Functional mapping and annotation of genetic associations with FUMA. *Nature Communications* **8**, 1826 (2017).
61. Jansen, P.R. *et al.* Genome-wide analysis of insomnia in 1,331,010 individuals identifies new risk loci and functional pathways. *Nature Genetics* **51**, 394-403 (2019).
62. Skol, A.D., Scott, L.J., Abecasis, G.R. & Boehnke, M. Joint analysis is more efficient than replication-based analysis for two-stage genome-wide association studies. *Nature Genetics* **38**, 209-213 (2006).
63. Jansen, I.E. *et al.* Genome-wide meta-analysis identifies new loci and functional pathways influencing Alzheimer's disease risk. *Nature genetics* **51**, 404-413 (2019).

64. Buniello, A. *et al.* The NHGRI-EBI GWAS Catalog of published genome-wide association studies, targeted arrays and summary statistics 2019. *Nucleic Acids Research* **47**, D1005-D1012 (2018).
65. Edwards, T.L. *et al.* Genome-wide association study confirms SNPs in SNCA and the MAPT region as common risk factors for Parkinson disease. *Annals of Human Genetics* **74**, 97-109 (2010).
66. Pickrell, J.K. *et al.* Detection and interpretation of shared genetic influences on 42 human traits. *Nature genetics* **48**, 709 (2016).
67. Consortium, I.P.D.G. Imputation of sequence variants for identification of genetic risks for Parkinson's disease: a meta-analysis of genome-wide association studies. *The Lancet* **377**, 641-649 (2011).
68. Vacic, V. *et al.* Genome-wide mapping of IBD segments in an Ashkenazi PD cohort identifies associated haplotypes. *Human molecular genetics* **23**, 4693-4702 (2014).
69. Pankratz, N. *et al.* Meta-analysis of Parkinson's disease: identification of a novel locus, RIT2. *Annals of neurology* **71**, 370-384 (2012).
70. Caligiore, D. *et al.* Parkinson's disease as a system-level disorder. *npj Parkinson's Disease* **2**, 1-9 (2016).
71. Bernardinis, M., Atashzar, S.F., Jog, M.S. & Patel, R.V. Differential Temporal Perception Abilities in Parkinson's Disease Patients Based on Timing Magnitude. *Scientific reports* **9**, 1-16 (2019).
72. Rowe, J. *et al.* Attention to action in Parkinson's disease: impaired effective connectivity among frontal cortical regions. *Brain* **125**, 276-289 (2002).
73. Jun, G. *et al.* A novel Alzheimer disease locus located near the gene encoding tau protein. *Molecular Psychiatry* **21**, 108-117 (2016).
74. Kouri, N. *et al.* Genome-wide association study of corticobasal degeneration identifies risk variants shared with progressive supranuclear palsy. *Nature communications* **6**, 7247 (2015).
75. Höglinger, G.U. *et al.* Identification of common variants influencing risk of the tauopathy progressive supranuclear palsy. *Nature genetics* **43**, 699 (2011).
76. Grove, J. *et al.* Identification of common genetic risk variants for autism spectrum disorder. *Nature genetics* **51**, 431 (2019).

77. Nagel, M. *et al.* Meta-analysis of genome-wide association studies for neuroticism in 449,484 individuals identifies novel genetic loci and pathways. *Nature Genetics* **50**, 920 (2018).
78. Lee, J.J. *et al.* Gene discovery and polygenic prediction from a genome-wide association study of educational attainment in 1.1 million individuals. *Nature Genetics* **50**, 1112–1121 (2018).
79. Kichaev, G. *et al.* Leveraging polygenic functional enrichment to improve GWAS power. *The American Journal of Human Genetics* **104**, 65-75 (2019).
80. Davies, G. *et al.* Genome-wide association study of cognitive functions and educational attainment in UK Biobank (N= 112 151). *Molecular Psychiatry* **21**, 758–767 (2016).
81. Dashti, H. *et al.* GWAS in 446,118 European adults identifies 78 genetic loci for self-reported habitual sleep duration supported by accelerometer-derived estimates. *bioRxiv*, 274977 (2018).
82. Morris, J.A. *et al.* An atlas of genetic influences on osteoporosis in humans and mice. *Nature genetics* **51**, 258 (2019).
83. Sanchez-Roige, S. *et al.* Genome-wide association study meta-analysis of the Alcohol Use Disorders Identification Test (AUDIT) in two population-based cohorts. *American Journal of Psychiatry*, appi. ajp. 2018.18040369 (2018).
84. Jun, G.R. *et al.* Transethnic genome-wide scan identifies novel Alzheimer's disease loci. *Alzheimer's & Dementia* **13**, 727-738 (2017).
85. Nazarian, A., Yashin, A.I. & Kulminski, A.M. Genome-wide analysis of genetic predisposition to Alzheimer's disease and related sex disparities. *Alzheimer's research & therapy* **11**, 5 (2019).
86. Ramanan, V.K. *et al.* APOE and BCHE as modulators of cerebral amyloid deposition: a florbetapir PET genome-wide association study. *Molecular psychiatry* **19**, 351-357 (2014).
87. Harold, D. *et al.* Genome-wide association study identifies variants at CLU and PICALM associated with Alzheimer's disease. *Nature genetics* **41**, 1088 (2009).
88. Scelsi, M.A. *et al.* Genetic study of multimodal imaging Alzheimer's disease progression score implicates novel loci. *Brain* **141**, 2167-2180 (2018).

89. Ferrari, R. *et al.* A genome-wide screening and SNPs-to-genes approach to identify novel genetic risk factors associated with frontotemporal dementia. *Neurobiology of aging* **36**, 2904. e13-2904. e26 (2015).
90. Beecham, G.W. *et al.* Genome-wide association meta-analysis of neuropathologic features of Alzheimer's disease and related dementias. *PLoS Genet* **10**, e1004606 (2014).
91. Davies, G. *et al.* A genome-wide association study implicates the APOE locus in nonpathological cognitive ageing. *Molecular Psychiatry* **19**, 76-87 (2014).
92. Zhang, C. & Pierce, B.L. Genetic susceptibility to accelerated cognitive decline in the US Health and Retirement Study. *Neurobiology of aging* **35**, 1512. e11-1512. e18 (2014).
93. Raj, T. *et al.* Genetic architecture of age-related cognitive decline in African Americans. *Neurology Genetics* **3**(2017).
94. Liu, C. *et al.* Genome-wide association and mechanistic studies indicate that immune response contributes to Alzheimer's disease development. *Frontiers in genetics* **9**, 410 (2018).
95. Yan, Q. *et al.* Genome-wide association study of brain amyloid deposition as measured by Pittsburgh Compound-B (PiB)-PET imaging. *Molecular psychiatry*, 1-13 (2018).
96. Liang, P. *et al.* Altered amplitude of low-frequency fluctuations in early and late mild cognitive impairment and Alzheimer's disease. *Current Alzheimer Research* **11**, 389-398 (2014).
97. Liu, X. *et al.* Abnormal amplitude of low-frequency fluctuations of intrinsic brain activity in Alzheimer's disease. *Journal of Alzheimer's Disease* **40**, 387-397 (2014).
98. Mattsson, N. *et al.* Emerging β-amyloid pathology and accelerated cortical atrophy. *JAMA neurology* **71**, 725-734 (2014).
99. Pardiñas, A.F. *et al.* Common schizophrenia alleles are enriched in mutation-intolerant genes and in regions under strong background selection. *Nature Genetics* **50**, 381–389 (2018).
100. Hyde, C.L. *et al.* Identification of 15 genetic loci associated with risk of major depression in individuals of European descent. *Nature genetics* **48**, 1031 (2016).

101. Howard, D.M. *et al.* Genome-wide meta-analysis of depression identifies 102 independent variants and highlights the importance of the prefrontal brain regions. *Nature neuroscience* **22**, 343 (2019).

102. Anney, R.J. *et al.* Meta-analysis of GWAS of over 16,000 individuals with autism spectrum disorder highlights a novel locus at 10q24. 32 and a significant overlap with schizophrenia. *Molecular Autism* **8**, 21 (2017).

103. Baselmans, B.M. *et al.* Multivariate genome-wide analyses of the well-being spectrum. *Nature genetics* **51**, 445-451 (2019).

104. Lane, J.M. *et al.* Biological and clinical insights from genetics of insomnia symptoms. *Nature genetics* **51**, 387-393 (2019).

105. Hill, W. *et al.* A combined analysis of genetically correlated traits identifies 187 loci and a role for neurogenesis and myelination in intelligence. *Molecular Psychiatry* **24**, 169–181 (2019).

106. van der Meer, D. *et al.* Brain scans from 21,297 individuals reveal the genetic architecture of hippocampal subfield volumes. *Molecular Psychiatry*, in press. (2018).

107. Supekar, K., Cai, W., Krishnadas, R., Palaniyappan, L. & Menon, V. Dysregulated brain dynamics in a triple-network saliency model of schizophrenia and its relation to psychosis. *Biological psychiatry* **85**, 60-69 (2019).

108. Zheng, H. *et al.* The altered triple networks interaction in depression under resting state based on graph theory. *BioMed research international* **2015**.

109. Uddin, L.Q. *et al.* Salience network–based classification and prediction of symptom severity in children with autism. *JAMA psychiatry* **70**, 869-879 (2013).

110. Ripke, S. *et al.* Biological insights from 108 schizophrenia-associated genetic loci. *Nature* **511**, 421 (2014).

111. Liu, M. *et al.* Association studies of up to 1.2 million individuals yield new insights into the genetic etiology of tobacco and alcohol use. *Nature genetics* **51**, 237-244 (2019).

112. Jones, S.E. *et al.* Genome-wide association analyses of chronotype in 697,828 individuals provides insights into circadian rhythms. *Nature communications* **10**, 343 (2019).

113. Davies, G. *et al.* Study of 300,486 individuals identifies 148 independent genetic loci influencing general cognitive function. *Nature Communications* **9**, 2098 (2018).
114. Savage, J.E. *et al.* Genome-wide association meta-analysis in 269,867 individuals identifies new genetic and functional links to intelligence. *Nature Genetics* **50**, 912-919 (2018).
115. Kemp, J.P. *et al.* Identification of 153 new loci associated with heel bone mineral density and functional involvement of GPC6 in osteoporosis. *Nature genetics* **49**, 1468 (2017).
116. Chauhan, G. *et al.* Identification of additional risk loci for stroke and small vessel disease: a meta-analysis of genome-wide association studies. *The Lancet Neurology* **15**, 695-707 (2016).
117. Malik, R. *et al.* Multiancestry genome-wide association study of 520,000 subjects identifies 32 loci associated with stroke and stroke subtypes. *Nature genetics* **50**, 524-537 (2018).
118. Bulik-Sullivan, B. *et al.* An atlas of genetic correlations across human diseases and traits. *Nature Genetics* **47**, 1236-1241 (2015).
119. Zhao, B. *et al.* Common genetic variation influencing human white matter microstructure. *bioRxiv* (2020).
120. Qing, Z. & Gong, G. Size matters to function: brain volume correlates with intrinsic brain activity across healthy individuals. *Neuroimage* **139**, 271-278 (2016).
121. Okada, N. *et al.* Abnormal asymmetries in subcortical brain volume in schizophrenia. *Molecular psychiatry* **21**, 1460-1466 (2016).
122. Levitt, J.J. *et al.* MRI study of caudate nucleus volume and its cognitive correlates in neuroleptic-naive patients with schizotypal personality disorder. *American Journal of Psychiatry* **159**, 1190-1197 (2002).
123. Schaefer, A. *et al.* Local-global parcellation of the human cerebral cortex from intrinsic functional connectivity MRI. *Cerebral cortex* **28**, 3095-3114 (2018).
124. Fjell, A.M. *et al.* Relationship between structural and functional connectivity change across the adult lifespan: a longitudinal investigation. *Human brain mapping* **38**, 561-573 (2017).

125. Consortium, C.-D.G.o.t.P.G. Identification of risk loci with shared effects on five major psychiatric disorders: a genome-wide analysis. *The Lancet* **381**, 1371-1379 (2013).
126. Meng, X. *et al.* Increased Dynamic Amplitude of Low Frequency Fluctuation in Primary Insomnia. *Frontiers in Neurology* **11**, 609 (2020).
127. Liu, X. *et al.* Altered intrinsic coupling between functional connectivity density and amplitude of low-frequency fluctuation in mild cognitive impairment with depressive symptoms. *Neural plasticity* **2018**.
128. Golkar, A. *et al.* The influence of work-related chronic stress on the regulation of emotion and on functional connectivity in the brain. *PLoS One* **9**, e104550 (2014).
129. Kullmann, S. *et al.* The obese brain: association of body mass index and insulin sensitivity with resting state network functional connectivity. *Human brain mapping* **33**, 1052-1061 (2012).
130. Shokri-Kojori, E., Tomasi, D., Wiers, C.E., Wang, G.-J. & Volkow, N.D. Alcohol affects brain functional connectivity and its coupling with behavior: greater effects in male heavy drinkers. *Molecular psychiatry* **22**, 1185-1195 (2017).
131. Zhou, S. *et al.* Effect of smoking on resting-state functional connectivity in smokers: A n fMRI study. *Respirology* **22**, 1118-1124 (2017).
132. de Leeuw, C.A., Mooij, J.M., Heskes, T. & Posthuma, D. MAGMA: generalized gene-set analysis of GWAS data. *PLoS Computational Biology* **11**, e1004219 (2015).
133. Atkinson-Clement, C., Pinto, S., Eusebio, A. & Coulon, O. Diffusion tensor imaging in Parkinson's disease: review and meta-analysis. *Neuroimage: Clinical* **16**, 98-110 (2017).
134. Muralidharan, A. *et al.* Physiological changes in the pallidum in a progressive model of Parkinson's disease: Are oscillations enough? *Experimental neurology* **279**, 187-196 (2016).
135. Criaud, M. *et al.* Contribution of insula in Parkinson's disease: A quantitative meta-analysis study. *Human brain mapping* **37**, 1375-1392 (2016).
136. Wang, Q. *et al.* A Bayesian framework that integrates multi-omics data and gene networks predicts risk genes from schizophrenia GWAS data. *Nature neuroscience* **22**, 691 (2019).

137. Axelrud, L.K. *et al.* Genetic risk for Alzheimer's disease and functional brain connectivity in children and adolescents. *Neurobiology of aging* **82**, 10-17 (2019).
138. Karch, C.M. & Goate, A.M. Alzheimer's disease risk genes and mechanisms of disease pathogenesis. *Biological psychiatry* **77**, 43-51 (2015).
139. Zhu, Z., Lin, Y., Li, X., Driver, J.A. & Liang, L. Shared genetic architecture between metabolic traits and Alzheimer's disease: a large-scale genome-wide cross-trait analysis. *Human genetics* **138**, 271-285 (2019).
140. Varma, V.R. *et al.* Brain and blood metabolite signatures of pathology and progression in Alzheimer disease: A targeted metabolomics study. *PLoS medicine* **15**, e1002482 (2018).
141. Finucane, H.K. *et al.* Partitioning heritability by functional annotation using genome-wide association summary statistics. *Nature genetics* **47**, 1228-1235 (2015).
142. Kundaje, A. *et al.* Integrative analysis of 111 reference human epigenomes. *Nature* **518**, 317 (2015).
143. Fullard, J.F. *et al.* An atlas of chromatin accessibility in the adult human brain. *Genome research* **28**, 1243-1252 (2018).
144. Aguet, F. *et al.* The GTEx Consortium atlas of genetic regulatory effects across human tissues. *BioRxiv*, 787903 (2019).
145. Uribe-Bojanini, E., Hernandez-Quiceno, S. & Cock-Rada, A.M. Xeroderma Pigmentosum with Severe Neurological Manifestations/De Sanctis–Cacchione Syndrome and a Novel XPC Mutation. *Case reports in medicine* **2017**(2017).
146. Kraemer, K.H. *et al.* Xeroderma pigmentosum, trichothiodystrophy and Cockayne syndrome: a complex genotype–phenotype relationship. *Neuroscience* **145**, 1388-1396 (2007).
147. Wu, M. *et al.* Identification of key genes and pathways for Alzheimer's disease via combined analysis of genome-wide expression profiling in the hippocampus. *Biophysics Reports* **5**, 98-109 (2019).
148. Huntenburg, J.M. *et al.* A systematic relationship between functional connectivity and intracortical myelin in the human cerebral cortex. *Cerebral Cortex* **27**, 981-997 (2017).

149. Anttinen, A. *et al.* Neurological symptoms and natural course of xeroderma pigmentosum. *Brain* **131**, 1979-1989 (2008).
150. Bycroft, C. *et al.* The UK Biobank resource with deep phenotyping and genomic data. *Nature* **562**, 203-209 (2018).
151. Jiang, L. *et al.* A resource-efficient tool for mixed model association analysis of large-scale data. *Nature genetics* **51**, 1749 (2019).
152. Purcell, S. *et al.* PLINK: a tool set for whole-genome association and population-based linkage analyses. *The American Journal of Human Genetics* **81**, 559-575 (2007).
153. Willer, C.J., Li, Y. & Abecasis, G.R. METAL: fast and efficient meta-analysis of genomewide association scans. *Bioinformatics* **26**, 2190-2191 (2010).
154. Consortium, I.H. Integrating common and rare genetic variation in diverse human populations. *Nature* **467**, 52-58 (2010).
155. Liberzon, A. *et al.* Molecular signatures database (MSigDB) 3.0. *Bioinformatics* **27**, 1739-1740 (2011).

METHODS

Imaging phenotypes and datasets. The rsfMRI datasets were consistently processed following the procedures in UK Biobank imaging pipeline[10]. Details about image acquisition, preprocessing, and phenotype generation in each dataset can be found in **Supplementary Note**. Following the previous study[37], we generated two groups of phenotypes, including 76 node amplitude traits reflecting the spontaneous neuronal activity, 1,695 pairwise functional connectivity traits quantifying co-activity for node pairs, and 6 global functional connectivity measures to summarize all pairwise functional connectivity (**Supplementary Table 21**). For each continuous phenotype or covariate variable, values greater than five times the median absolute deviation from the median value were removed. We analyzed the following datasets separately: 1) the UKB discovery GWAS, which used data of individuals of British ancestry[150] in the UKB study (n = 34,691); 2) four European validation GWAS: UKB White but Non-British (UKBW, n = 1,970), ABCD European (ABCDE, n = 3,821), HCP (n = 495), and PNC (n = 510); 3) two non-European UKB validation GWAS: UKB Asian (UKBA, n = 446) and UKB Black (UKBBL, n = 232); and 4) two non-European non-UKB validation GWAS, including ABCD Hispanic

(ABCDH, *n* = 768) and ABCD African American (ABCDA, *n* = 1,257). See **Supplementary Table 22** for a summary of these datasets and demographic information. The assignment of ancestry in UKB was based on self-reported ethnicity (Data-Field 21000), which was verified in Bycroft, et al. [150]. The ancestry in ABCD was assigned by combining the self-reported ethnicity and ancestry inference results as in Zhao, et al. [119]. The functional brain regions characterized in ICA were labelled using the automated anatomical labeling atlas[57] (**Supplementary Table 23**) and were mapped onto major RSNs defined in Yeo, et al. [19] and Finn, et al. [17] (**Supplementary Figs. 12-13, Supplementary Tables 24-26**). Details of mapping procedures can be found in **Supplementary Note**.

GWAS discovery and validation. Details of genotyping and quality controls can be found in **Supplementary Note**. SNP heritability was estimated by GCTA[58] using all autosomal SNPs in the UKB British cohort. We adjusted the effects of age (at imaging), age-squared, sex, age-sex interaction, age-squared-sex interaction, imaging site, and the top 40 genetic principle components (PCs). Genome-wide association analysis was performed in linear mixed effect model using fastGWA[151], while adjusting the same set of covariates as in GCTA. GWAS were also separately performed via Plink[152] in European validation datasets UKBW, ABCDE, HCP, and PNC, where the effects of age, age-squared, sex, imaging sites (if applicable), age-sex interaction, age-squared-sex interaction, and top ten genetic PCs were adjusted.

To validate results in the UKB British discovery GWAS, meta-analysis was performed using the sample-size weighted approach via METAL[153]. We checked whether the locus-level associations detected in the British GWAS can be validated in the meta-analyzed GWAS. We also performed meta-analysis for the UKB British discovery GWAS and the meta-analyzed validation GWAS to check whether the *P*-values became smaller after combining these results. Polygenic risk scores (PRS) were constructed on eight validation datasets using Plink. The BLUP effect sizes estimated from GCTA-GREML analysis in UKB British discovery GWAS were used as weights in PRS construction, which accounted for the LD structures. Ambiguous variants (i.e. variants with complementary alleles) were removed from analysis. We tried 17 *P*-value thresholds for variant

selection according to their marginal *P*-values from fastGWA: 1, 0.8, 0.5, 0.4, 0.3, 0.2, 0.1, 0.08, 0.05, 0.02, 0.01, 1×10^{-3}, 1×10^{-4}, 1×10^{-5}, 1×10^{-6}, 1×10^{-7}, and 1×10^{-8}. The best prediction accuracy achieved by a single threshold was reported for each phenotype, which was measured by the additional phenotypic variation that can be explained by the polygenic profile (i.e., the incremental R-squared), adjusting for the effects of age, gender, and top ten genetic PCs.

The shared loci and genetic correlation. The genomic loci associated with intrinsic brain activity traits were defined using FUMA (version 1.3.5e). We input UKB British discovery summary statistics after reweighting the *P*-values using functional information via FINDOR[79]. After LD-based clumping, FUMA identified independent significant variants, which were defined as variants with a *P*-value smaller than the predefined threshold and were independent of other significant variants (LD $r^2 < 0.2$). FUMA then constructed LD blocks for these independent significant variants by tagging all variants in LD ($r^2 \geq 0.6$) with at least one independent significant variant and had a MAF ≥ 0.0005. These variants included those from the 1000 Genomes reference panel that may not have been included in the GWAS. Moreover, within these significant variants, independent lead variants were identified as those that were independent from each other (LD $r^2 < 0.1$). If LD blocks of independent significant variants were close (<250 kb based on the closest boundary variants of LD blocks), they were merged into a single genomic locus. Thus, each genomic locus could contain multiple significant variants and lead variants. Independent significant variants and all the variants in LD with them ($r^2 \geq 0.6$) were searched by FUMA on the NHGRI-EBI GWAS catalog (version 2019-09-24) to look for previously reported associations ($P < 9 \times 10^{-6}$) with any traits. LDSC[118] software (version 1.0.1) was used to estimate and test the pairwise genetic correlation. We used the pre-calculated LD scores provided by LDSC, which were computed using 1000 Genomes European data. We used HapMap3[154] variants and removed all variants in the major histocompatibility complex (MHC) region. The summary statistics of intrinsic brain activity traits were from the UKB British discovery GWAS and the resources of other summary statistics were provided in **Supplementary Table 10**.

Gene-level analysis and biological annotation. Gene-based association analysis was performed in UKB British participants for 18,796 protein-coding genes using MAGMA[132] (version 1.07). Default MAGMA settings were used with zero window size around each gene. We then carried out FUMA functional annotation and mapping analysis, in which variants were annotated with their biological functionality and then were linked to 35,808 candidate genes by a combination of positional, eQTL, and 3D chromatin interaction mappings. Brain-related tissues/cells were selected in all options and default values were used for all other parameters in FUMA. For the detected genes in MAGMA and FUMA, we performed lookups in the NHGRI-EBI GWAS catalog (version 2020-02-08) to explore their previously reported gene-trait associations. We performed heritability enrichment analysis via partitioned LDSC[141]. Baseline models were adjusted when estimating and testing the enrichment scores for our tissue type and cell type specific annotations. Methods to analysis chromatin data of glial and neuronal cell subtypes can be found in Zhao, et al. [119]. We also performed gene property analysis for the 13 GTEx[144] v8 brain tissues via MAGMA. Specifically, we examined whether the tissue-specific gene expression levels can be linked to the strength of the gene-trait association. MAGMA was also used to explore the enriched biological pathways, in which we tested 500 curated gene sets and 9,996 Gene Ontology (GO) terms from the Molecular Signatures Database[155] (MSigDB, version 7.0).

Code availability

We made use of publicly available software and tools listed in URLs. Other codes used in our analyses are available upon reasonable request.

Data availability

Our GWAS summary statistics can be downloaded at https://github.com/BIG-S2/GWAS. The individual-level data used in the present study can be obtained from four publicly accessible data resources: UK Biobank (http://www.ukbiobank.ac.uk/resources/), ABCD (https://abcdstudy.org/), HCP (https://www.humanconnectome.org/), and PNC (https://www.med.upenn.edu/bbl/philadelphianeurodevelopmentalcohort.html). Our results can also be easily browsed through our knowledge portal https://bigkp.web.unc.edu/.

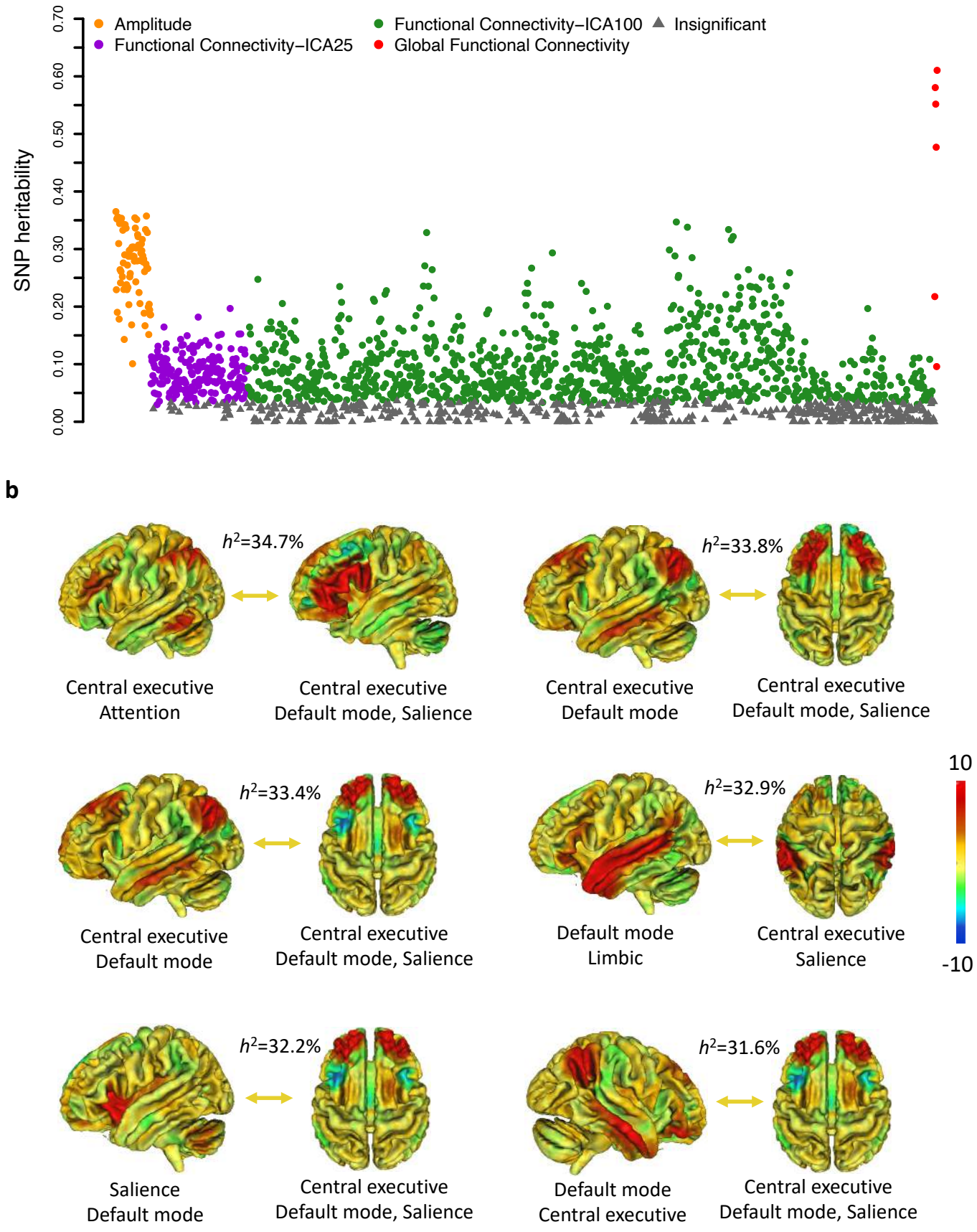

Figure 1: SNP heritability estimates of intrinsic brain activity (n = 34,691 subjects). **a**) The SNP heritability estimates of 1,777 intrinsic brain activity traits, including 76 amplitude traits, 1,695 pairwise functional connectivity traits, and 6 global functional connectivity measures. Two parcellations with different dimensionalities (25 and 100, respectively) were applied. **b**) The 6 pairwise functional connectivity traits that had heritability larger than 30%.

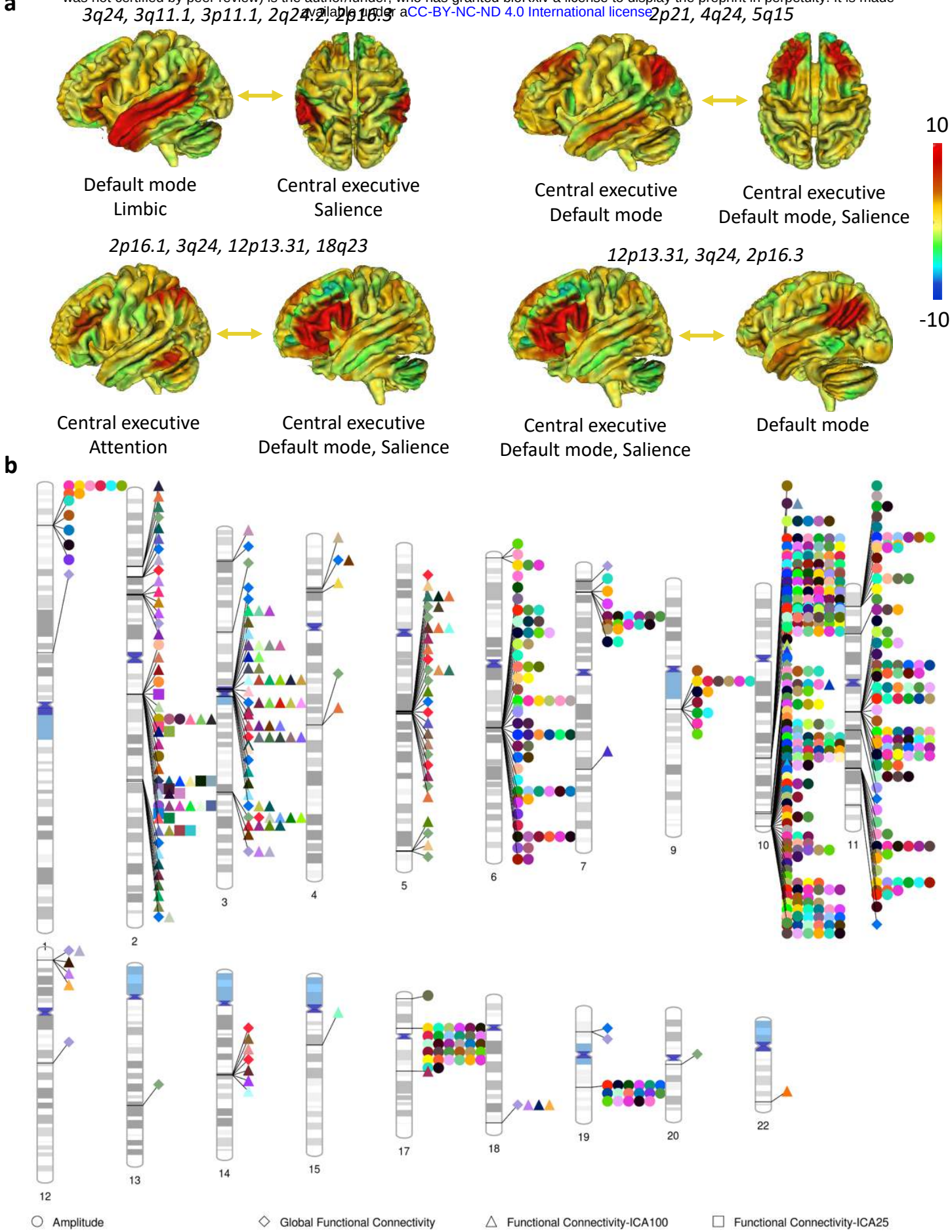

Figure 2: The associated genetic loci of intrinsic brain activity (n = 34,691 subjects). **a**) Selected pairwise functional connectivity traits that had multiple associated genetic loci. **b**) Ideogram of all loci influencing intrinsic brain activity.

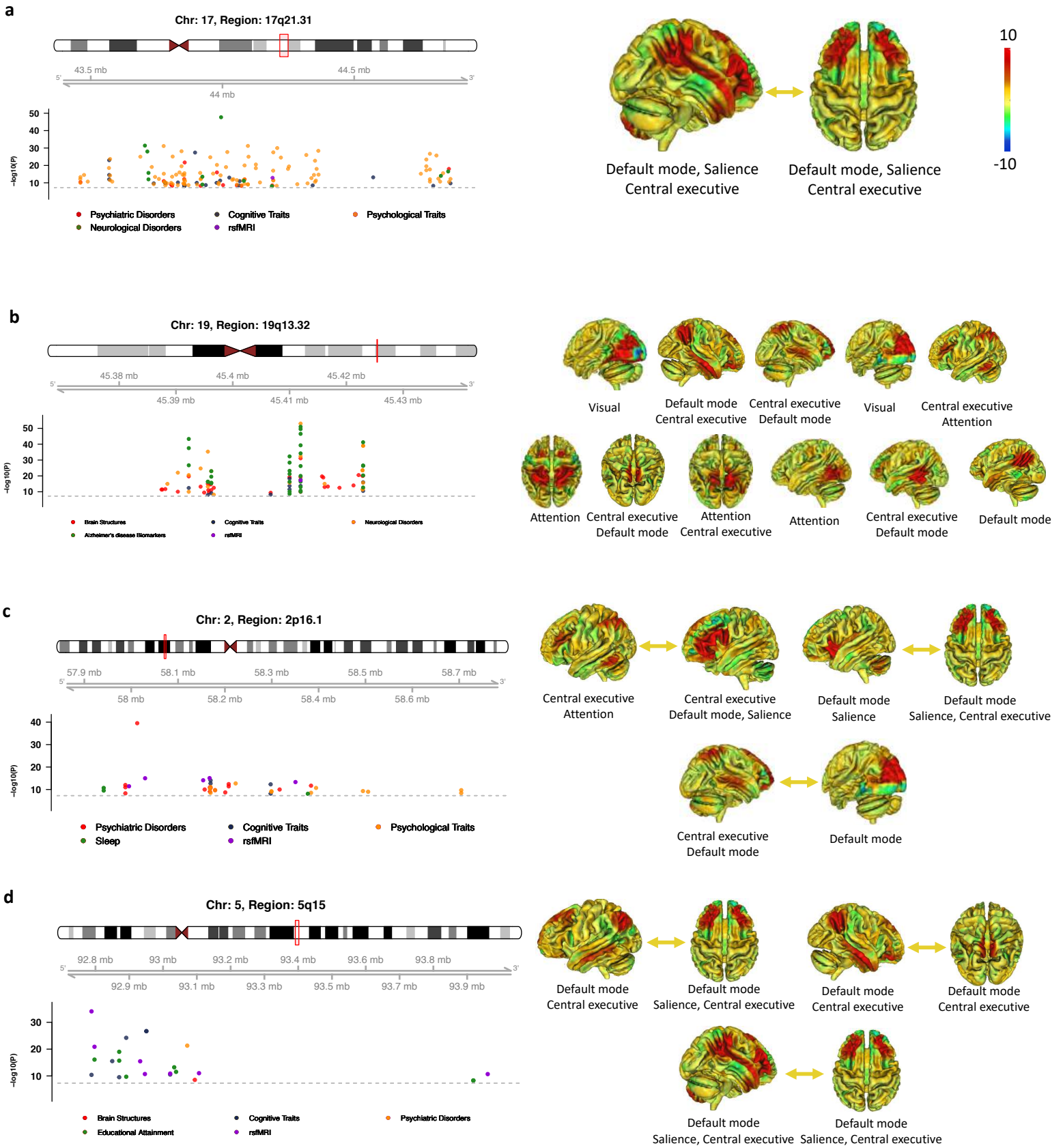

Figure 3: The selected shared loci associated with both intrinsic brain activity and other brain-related complex traits and disorders. We illustrate local colocalizations (left, LD $r^2 \geq 0.6$) between intrinsic brain activity traits (right) associated variants (n = 34,691 subjects) and previously reported associations of other traits on the NHGRI-EBI GWAS catalog (https://www.ebi.ac.uk/gwas/).

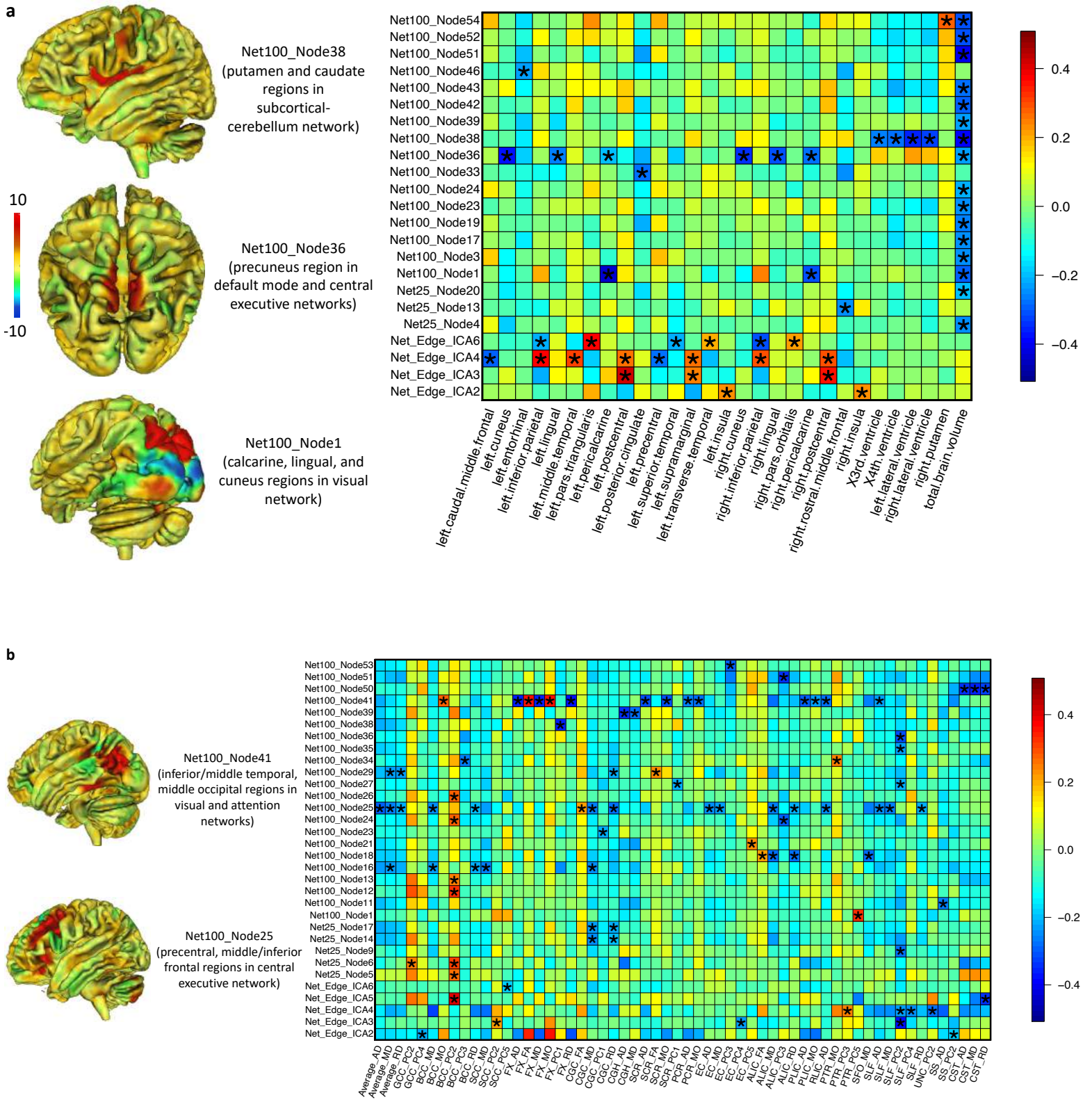

Figure 4: Pairwise genetic correlations between intrinsic brain activity and brain structure (n = 34,691 subjects). a) Genetic correlations between intrinsic brain activity traits and regional brain volumes. **b)** Genetic correlations between intrinsic brain activity traits and DTI traits of white matter microstructure. The x axis lists names of brain structural traits and y axis lists names of brain intrinsic brain activity traits. We adjusted for multiple testing by the Benjamini-Hochberg procedure at 0.05 significance level (82×315 tests), while significant pairs are labeled with stars.

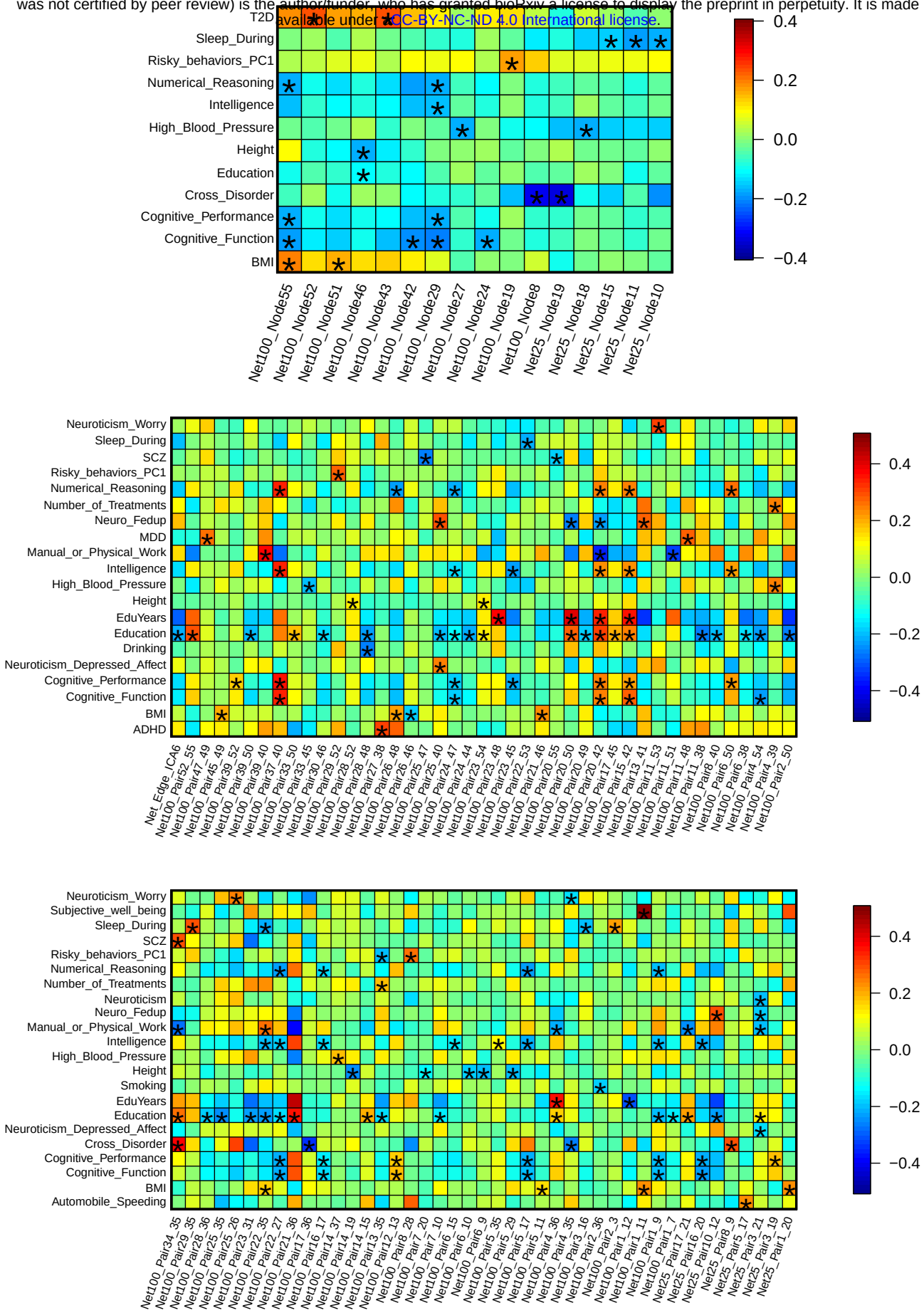

Figure 5: Pairwise genetic correlations between intrinsic brain activity and other complex traits (n = 34,691 subjects). We adjusted for multiple testing by the Benjamini-Hochberg procedure at 0.05 significance level ($1,777 \times 30$ tests), while significant pairs are labeled with stars. The y axis lists names of brain structural traits and x axis lists names of other complex traits.